JOURNAL OF OPTOELECTRONICS AND ADVANCED MATERIALS Vol. 10, No. 7, July 2008, p. 1885 - 1888

# Low temperature chemical synthesis of Ni-Zn ferrite nanoparticles

B. PARVATHEESWARA RAO[a,c] O. F. CALTUN[a], CHEOLGI KIM[*c]
[a]*Department of Physics, Andhra University, Visakhapatnam 530003, India*
[b]*Faculty of Physics, A.I. Cuza University, Iasi, 700506 Romania*
[c]*Research Center for Advanced Magnetic Materials, Chungnam National University, Daejeon, Korea*

Ferrite nanoparticles of the composition $Ni_{0.65}$ $Zn_{0.35}$ $Fe_2$ $O_4$ were prepared by low temperature sol-gel synthesis method using metal nitrates in poly vinyl alcohol (PVA) and in citric acid (CA) matrixes independently to estimate the influence of synthesis matrix on the structural and magnetic parameters of this high saturation magnetization Ni-Zn ferrite composition. Appropriate amounts of metal nitrates were dissolved first in minimum amounts of deionized water to produce clear cationic solutions and then either PVA or CA was added in 1:1 ratio while stirring to form a highly viscous gel. The dried gels were then heat treated at 350 $^oC$ for 1h to find them burnt out in a self propagating combustion manner to form loose powders. The resulting powders were characterized by X-ray diffraction, transmission electron microscopy and vibrating sample magnetometer techniques. The sol-gel in PVA sample resulted in fine particle size while the sol-gel in citric acid sample displayed higher magnetization close to that of its bulk value. The lattice constant, magnetization and corecivity of these samples have a direct bearing with the corresponding average crystallite size. The results are analyzed in terms of the core-shell behaviour of the nanoparticles.

(Received April 1, 2008; accepted June 30, 2008)

*Keywords*: Ferrite nanoparticles, Magnetization, Particle size, Chemical synthesis

## 1. Introduction

Ferrites with useful electromagnetic properties offer inexpensive solutions to many applications over a wide frequency range [1]. Since there have been increasing demands for miniaturized yet high performance cores, development of ferrite materials at nanoscales would be expected to deliver fruitful results as they can function at high frequencies by avoiding domain wall resonance [2]. When the particle becomes sufficiently smaller, it exists in a single domain state and domain wall resonance can be avoided, and the resulting core can thus work at higher frequencies. Therefore, investigations of ferrite particles at nanoscales need to be carried out not only to meet the technological requirements but also to understand the physics behind the evolution of such magnetic transformations.

In the literature, soft chemical methods were mostly preferred for synthesis of nanoparticles as they provide better homogeneity and greater uniformity in particle size and size distribution. Among various methods of synthesis, sol-gel auto combustion methods with different matrixes, such as poly vinyl alcohol [3], citric acid [4], etc. are largely pursued due to their ease in execution and ability to prepare powders relatively in large quantities. However, a comparison of the structural and magnetic performance between these methods for a given system has not been reported so far. Therefore, in the present work, we focused on the preparation of Ni-Zn ferrite nanoparticles by two soft chemical methods, and the results of their structural and magnetic characterizations are closely examined, analyzed and reported here.

## 2. Experimental

The Ni-Zn ferrite system, $Ni_{0.65}$ $Zn_{0.35}$ $Fe_2$ $O_4$, has been chosen for the present study as this composition exhibits high saturation magnetizations in the entire Ni-Zn series and is a good candidate for power applications beyond 1 MHz. Synthesis of this system was carried out by sol-gel methods in poly vinyl alcohol, and in citric acid matrixes, separately. In both the methods, metal nitrates were taken as starting materials for making up cationic solutions. Appropriate amounts of metal nitrates were dissolved first in minimum amounts of deionized water to produce clear cationic solutions and then either poly vinyl alcohol (PVA) or citric acid (CA) was added in 1:1 ratio while stirring to form a highly viscous gel. These gels were then heated gradually up to 90 $^oC$ to evolve reddish brown gases and to become dried gels, which were finally heat treated at 350 $^oC$ for 1h to find out the dried gel burnt out in a self propagating combustion manner to form loose powders. The samples were subjected to X-ray diffraction, vibration sample magnetometry and transmission electron microscopy characterizations.

## 3. Results

The XRD patterns of both the ferrite nanoparticle systems are shown in fig. 1. All the peaks indicate single phase spinel crystal structure. However, it can be seen that the sol-gel in citric acid matrix shows better crystallinety with high intensities for all the peaks compared to sol-gel in PVA matrix for which the peaks appeared broader. Average crystallite size (D) of the

samples in each case was calculated from the broadening of the respective high intensity 311 peak using the Scherrer equation, $D=0.9\,\lambda / (\beta \cos\theta)$ [5], where $\lambda$ is the x-ray wavelength (1.5406 Å) and $\beta$ is the broadening of the peak at angle $\theta$. The $\beta$ is measured using the equation, $\beta = (B^2 - b_o^2)^{1/2}$, where B is the measured FWHM of the experimental profile and $b_o$ is the instrumental broadening. For the estimations, the peaks have been considered as voigt in shape and the data were best fitted to voigt. Though the composition is the same for both the samples, the average crystallite size is found to be larger for sol-gel CA method with 10.5 nm compared to 7.7 nm for sol-gel PVA method.

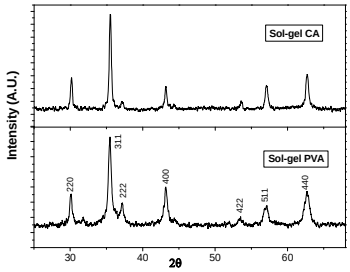


*Fig. 1. XRD patterns of sol-gel synthesized Ni-Zn ferrite*

Room temperature magnetic hysteresis loops of both the samples are shown in fig. 2. The samples have shown a clear hysteresis in each case. The observed magnetization values of these samples being 35.8 emu/g and 66.8 emu/g for sol-gel PVA and sol-gel CA methods, respectively are less than the magnetization value of the bulk sample (73 emu/g) of this composition [6]. The magnetization value of sol-gel CA sample with 10.5 nm has, however, come close to that of the bulk value. Apart from the magnetization, the coercivity values of these samples, being 61 and 71 Oe for sol-gel PVA and sol-gel CA samples, respectively have, however, shown a direct bearing with the average crystallite size.

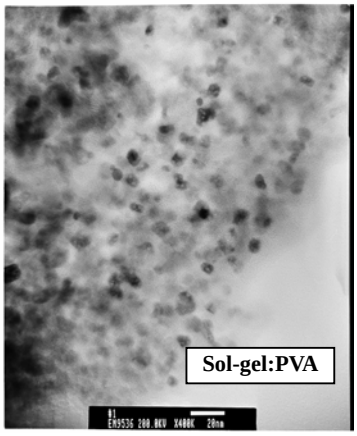


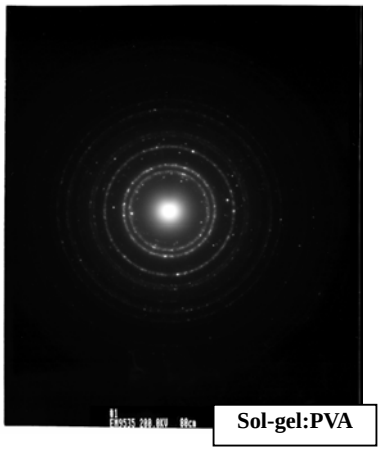


*nanoparticles*

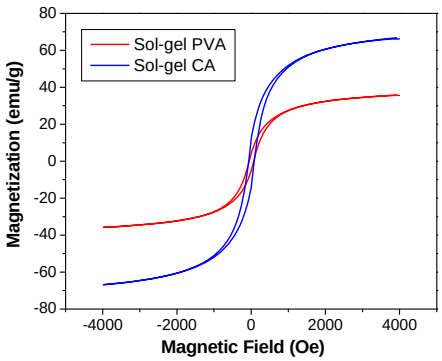


*Fig. 2. Hysteresis loops of sol-gel synthesized Ni-Zn ferrite nanoparticles*

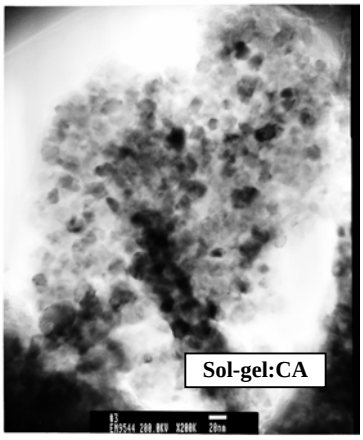


*Fig. 3. TEM images of $Ni_{0.65}\ Zn_{0.35}\ Fe_2\ O_4$ ferrite nanoparticles prepared under sol-gel CVA and sol-gel CA methods., and the selected area electron diffraction pattern of sol-gel PVA method.*

The TEM images of both the samples and the corresponding selected area electron diffraction pattern for sol-gel PVA are shown in fig.3. It is evident from the images that the synthesized particles are uniform and

well dispersed for both the sol-gel methods without any aggregates. Unfortunately, the particle sizes could not be deduced from the electron microscope used. However, visual examination of the particles based on the 20 nm scales in each case indirectly supports the estimations made by using Scherrer methods. Also, the faint intensity levels in the corresponding electron diffraction pattern for the sol-gel PVA sample may have connected to the lesser degree of crystalline nature as observed in X-ray diffraction patterns.

## 4. Discussion

Based on the peak central positions obtained from the best fits of high intensity low angle 311 and high angle 440 peaks, the lattice constant was estimated in each case and averaged out to represent the lattice constant of the sample. The corresponding values for sol-gel PVA and sol-gel CA are observed to be 8.3811 Å and 8.3873 Å, respectively. The lattice constant of the bulk $Ni_{0.65}$ $Zn_{0.35}$ $Fe_2$ $O_4$ prepared by conventional ceramic technique was reported to be ≈ 8.395 Å [7]. As can be observed, the estimated lattice constants in the present study are less than the value of their bulk counterpart. This deviation is found to be more if the average crystallite size is smaller. Deviations in lattice constant of the nanoparticles from their bulk were reported earlier too as due to enhanced lattices and interface structure with a large volume fraction in case of nanoparticles [8]. In another work, it was suggested that the decrease in lattice constant could be due to increased degree of inversion [9]. As the inversion degree increases, the relatively larger $Zn^{2+}$ ions in nanoparticle systems would migrate to B-sites from their conventionally preferred A-sites and comfortably occupy the larger octahedral interstices compared to the smaller tetrahedral interstices. Obviously, due to larger accommodation size in octahedral sites, the $Zn^{2+}$ ions need not have to push the oxygen ions around it to expand the lattice. If the $Zn^{2+}$ ions were in A-sites, they were normally assumed to push the oxygen ions around them and contribute to expand the lattice. Another probable reason for decrease in lattice constant in nanoparticles could be the high surface energy and surface tension. This results in a tendency to shrink the lattice which causes reduced lattice constants [9]. The observed deviations in lattice constant in the present study resulting in lower values as the particle size becomes smaller are attributed to the increased degree of inversion, more surface energy and tension related shrinking of the lattice.

In spinel ferrites, there were some attempts using the integrated intensity ratios of X-ray diffraction peaks on extracting the information related to cation distribution. The integrated intensity of (220) reflection is known to depend exclusively on the cations occupying A-sites, and the intensity of (222) reflection is to depend on the cations occupying B-sites only [10]. Therefore, any decrease in the intensity ratio of I(220)/I(222) means a reduction in the concentration of cations that fill the A-sites, and as a result equal number of cations, which could otherwise have filled the B-sites, would now migrate into A-sites and vice versa. In order to verify the migration of cations in the present study, the intensity ratios are estimated for both the samples and are observed to be 1.29 and 2.82 for sol-gel PVA and sol-gel CA methods, respectively. It is evident that the intensity ratio appears smaller for smaller average crystallite size. This implies increased migration of the A-site filled cations into B-sites as the size of the crystallites decreases. Though it could be a different story when the average crystallite size becomes larger beyond a threshold value [11], the present observations carry relevance for the simple reason that the estimated average crystallite sizes are small enough to lie below such threshold value for any deviation.

The super exchange interactions between the magnetic cations in spinel ferrites are antiferromagnetic. But, the ferrimagnetic order arises since the intersublattice exchange is stronger than the intrasublattice exchange. In the bulk regime, the investigated composition takes the distribution, such as $(Zn^{2+}_{0.35}\ Fe^{3+}_{0.65})\ [Ni^{2+}_{0.65}\ Fe^{3+}_{1.35}]\ O^{2-}_4$, which gives highest room temperature saturation magnetization among the $Ni_{1-x}$ $Zn_x$ $Fe_2$ $O_4$ system [7]. The cations figured in parenthesis and square brackets form tetrahedral and octahedral sublattices, respectively and the net magnetization in the optimal case is supposed to be obtained from the $Ni^{2+}$ ions and some $Fe^{3+}$ ions from the octahedral sublattice after compensating the $Fe^{3+}$ ions in the tetrahedral sublattice. If the same composition in nanoscale regime enforces a redistribution of the cations due to structural modifications, it is obvious that the resultant magnetization would be somewhat lesser from the highest value of the bulk regime. Literature find several reports [12-14] on ferrite nanoparticles demonstrating cation redistributions with higher degree of inversion due to surface disorder because of which there may be reduced coordination and broken exchange bonds between the surface spins. Further, as discussed earlier, for nanoparticles the surface areas are larger and thus the surface energy and surface tension are high. This results in changes in cationic preferences and leads to increased degree of inversion and thus lesser magnetizations. The observed smaller magnetizations in these samples, particularly for the sol-gel PVA sample with smaller average crystallite size, are in accordance with the arguments made above.

The coercivity values too in these samples reflect a typical particle size dependent behaviour [15]. As the particle size decreases, the coercivity increases to reach a maximum at a threshold particle size, which could be characteristically described as transformation from multi domain nature to single domain nature, and then decreases. The observed large values of coercivity for these samples reflect that they are far from superparamagnetic state and lie somewhere between single domain state to multi domain state.

## 5. Conclusions

X-ray diffraction patterns of the chemically synthesized Ni-Zn ferrite samples confirm single phase spinel structure. The average crystallite sizes of the samples point towards sol-gel PVA method for preferences of smaller particle sizes. From the integrated intensity ratio of X-ray diffraction peaks, it was observed an increase in the inversion degree of cation distribution as the particle size becomes smaller. The samples exhibit smaller magnetizations as the average crystallite size decreases and this was attributed to surface disorder and increased inversion degree. Among both the synthesis methods, the sol-gel method in citric acid matrix provides high degree of crystallinity with uniform microstructure and better magnetic behaviour.

**Acknowledgements**

Part of the work was supported by Brain Pool, Korea and DRDO, India.

## References

[1] A. C. Razzitte, S. E. Jacobo, J. Appl. Phys. **87**, 6232 (2000)
[2] Z. X. Tang, C. M. Sorensen, K. J. Klabunde, G.. C. Hadjipanayis, Phys. Rev. Lett., **67**, 3602 (1991).
[3] L. Wang, F. S. Li, J. Magn. Magn. Mater. **223**, 233 (2001).
[4] Z. Yue, Ji Zhou, L. Li, H. Zhang, Z. Gui, J. Magn. Magn. Mater. **208**, 55 (2000).
[5] B. D. Cullity, Elements of X-ray diffraction, 2nd ed. Addison-Wesley, Reading, MA, 1978.
[6] B. Parvatheeswara Rao, C. O. Kim, CheolGi Kim, I. Dumitru, L. Spinu, O. F. Caltun, IEEE trans. Magn. **42**, 2858 (2006).
[7] B. Parvatheeswara Rao, P.S.V. Subba Rao, K. H. Rao, IEEE trans. Magn. **33**, 4454 (1997).
[8] C. Upadhyay, H.C. Verma and S. Anand, J. Appl. Phys., **95**, 5746 (2004).
[9] S. D. Shenoy, P.A. Joy and M.R. Anantharaman, J. Magn. Magn. Mater., **269**, 217 (2004).
[10] V. Sepelak, D. Baabe, D. Mienert, D. Schultze, F. Krumeich, F.J. Litterst and K.D. Becker, J. Magn. Magn. Mater., **257**, 377 (2003).
[11] D. J. Fatemi, V. G. Harris, V. M. Browning, J. P. Kirkland, J. Appl. Phys., **83**, 6867 (1998).
[12] J. P. Chen, C. M. Sorensen, K. J. Klabunde, G. C. Hadjipanayis, E. Devlin, A. Kostikas, Phys. Rev. B, **54**, 9288 (1996).
[13] S. Calvin, E.E. Carpenter, B. Ravel, V.G. Harris, Phys. Rev. B **66**, 224405 (2002).
[14] M. George, S.S. Nair, A.M. John, P.A. Joy, M.R. Anantharaman, J.Phys.D: Appl. Phys. **39**, 900 (2006).
[15] M. Vucinic-Vasic, B. Antic, A. Kremenovic, A.S. Nikolic, M. Stoiljkovic, N. Bibic, V. Spasojevic Ph. Colomban, Nanotechnology **17**, 4877 (2006).

*Corresponding author: cgkim@cnu.ac.kr